Electronic Supplementary Information

Enhanced Proton Conductivity of Nafion Membrane Induced by Incorporation of MOFs-Anchored 3D Microspheres: A Superior and Promising Membrane for Fuel Cells Applications

Liyu Zhu,[a] Yucheng Li,[a] Jingyang Zhao,[a] Jing Liu,[a] Luying Wang,[a] Jiandu Lei,[a,b]* and Ruisheng Xue,[c]*

[a]Beijing Key Laboratory of Lignocellulosic Chemistry, Beijing Forestry University, Beijing 100083, China

[b]MOE Engineering Research Center of Forestry Biomass Materials and Bioenergy, Beijing Forestry University, Beijing 100083, China

[c]Beijing University of Chemical Technology, Beijing 100029, China

Corresponding Authors

*Email: ljd2012@bjfu.edu.cn (Jian-du Lei) and xuersh@mail.buct.edu.cn (Rui-sheng Xue)

Table of Contents

1. Materials and General Procedures

Materials: PCMs (Polyacrylate carboxyl microspheres) were purchased from SKB Sphere Technology Co., Ltd. 2-methylimidazole (99% purity) and Zinc nitrate hexahydrate (Zn $(NO_3)_2 \cdot 6H_2O$, 99% purity) were supplied from Sinopharm Chemical Reagent Co., Ltd. N, N-Dimethylacetamide (DMAc, >99% purity) was purchased from Shanghai Aladdin Bio-Chem Technology Co., Ltd. Nafion solution (20 wt%) was purchased from DuPont Co., Ltd. Methanol was provided by Beijing Chemical Plant.

Preparation of ZIF-8@PCMs. The ZIF-8@PCMs composites were synthesized by in-situ growth of ZIF-8 nanoparticles on the surface of PCMs (Fig. 2a). First, disperse 1.0 g PCMs powder into 100 mL methanol and 50 mL deionized water to obtain a uniform suspension. Then, 0.95 g Zn $(NO_3)_2 \cdot 6H_2O$ was dissolved in the above solution. The mixture was stirred in a thermostatic oscillator to promote the full coordination of Zn^{2+} with the carboxyl groups on PCMs at 30 ℃ for 24 h. Under the above experimental conditions, 4.5 g of 2-methylimidazole was dissolved in 50 mL of methanol solution and added to the above PCMs/Zn^{2+} suspension. After centrifugation and washing with methanol, the product was dried at 80 ℃ for 24 h to obtain ZIF-8 anchored PCMs.

Preparation of Nafion/ZIF-8@PCMs composite membranes. The Nafion/ZIF-8@PCMs composite membranes were prepared by the solution casting method [1]. First, the commercially available Nafion D-2020 dispersion (1.5 mL) was heated at 60 ℃ for 8 h to get dry Nafion resin, which was then dissolved in an appropriate amount of DMAc to form 0.045 g/mL Nafion/DMAc solution. Subsequently, different amounts of ZIF-8@PCMs were added into Nafion/DMAc solution to form a homogeneous polymer solution by stirring for 6 h and ultrasonic treatment for 1 h. Then, the Nafion/ZIF-8@PCMs mixture was poured onto a glass mold (8 cm×8 cm) and heated at 80 ℃ for 12 h. Finally, the membrane was then peeled from the glass plate, followed by being treated in 0.5 M sulfuric acid for 2 h. Additionally, the prepared

Nafion/ZIF-8@PCMs composite membranes were washed with deionized water before the characterizations. For simplicity, the notations of hybrid membranes with theoretical ZIF-8@PCMs content varied in 0.5, 1, 2, 4% (w/w) based on Nafion were denoted as ZIF-8@PCMs-X, where X represents the weight percentage of ZIF-8@PCMs in the Nafion matrix. The membrane thickness was controlled at 35±10 μm.

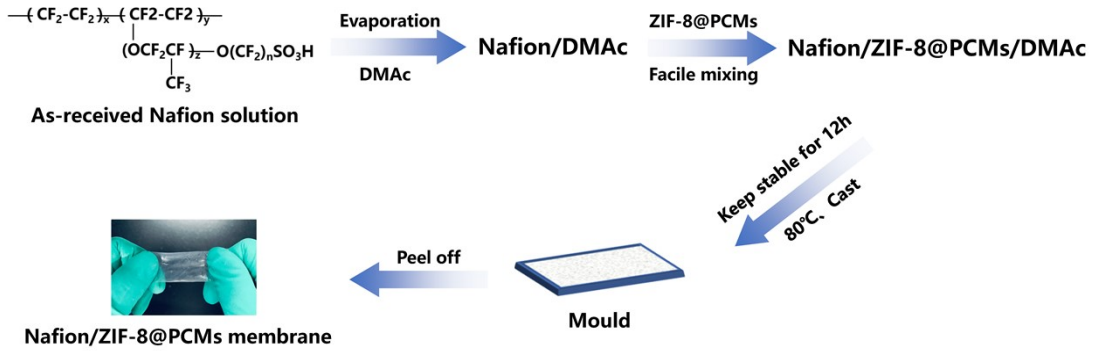

Fig. S1 Preparation procedures of Nafion/ZIF-8@PCMs composite membrane.

2. Characterizations

Characterizations of ZIF-8@PCMs. The morphology of ZIF-8, PCMs, and ZIF-8@PCMs was characterized by SEM. Element analysis was performed by SEM (ZEISS Gemini 300) equipped with an energy-dispersive spectrometer (EDS). X-ray diffraction (XRD) was obtained on Rigaku Ultima IV diffractometer with Cu-Kα radiation at the 2θ range of 5°-50°. Nitrogen adsorption isotherms of the membranes were measured on Micromeritics ASAP2460. Thermogravimetric analysis (TGA) was recorded on Perkin Elmer thermal analyzer (N_2 atmosphere).

Characterization of Nafion/ZIF-8@PCMs composite membranes. The morphology of the as-prepared membranes was observed by SEM (ZEISS Gemini 300). TGA was carried out using a TG-DTA8122 Thermal Analyzer (N_2 atmosphere) in the temperature range of 30-700℃ with a heating rate of 10 ℃/min. XRD was carried on a Rigaku Ultima IV in the ranges of 5-60°. An electromechanical universal testing machine (Instron 5943) was used to obtain the mechanical properties of the as-prepared membrane at 2 mm/min tensile speed. Three replicates of each sample were

tested to reduce the error. The oxidative stability was assessed using a Fenton reagent (3 wt% H_2O_2, 2 ppm $FeSO_4$) at 60 ℃.

The water uptake (WU) of the membranes was measured at 30 ℃ in water. The length and width of the membranes were measured and noted. Subsequently, the saturated membranes were re-weighted after removing the surface-adsorbed water by filter paper. Then they were weighted (M_{wet}) and calculated the area (A_{wet}). After drying in a vacuum oven at 80 ℃ for 12 h, the membranes were weighted and measured again and noted as M_{dry} and A_{dry}. Each measurement was repeated three times and averaged, which is obtained by using equation (1) and (2):

$$Water\ uptake(\%) = \frac{M_{wet} - M_{dry}}{M_{dry}} \times 100\% \quad (1)$$

$$Swelling\ degree\ (\%) = \frac{A_{wet} - A_{dry}}{A_{dry}} \times 100\% \quad (2)$$

The ion exchange capacity (IEC) was obtained by titration.[2] A measured amount of dried membranes (about 0.2 g) were immersed in 30 mL saturated NaCl solution to fully release H^+ ions into the solution at 60 °C for 24 h. After removing the membrane, the residual liquid on the membrane surface was flushed into the immersed NaCl solution with deionized water. The NaCl solution was titrated to neutral with 0.01 M NaOH solution using phenolphthalein as an indicator. The IEC values were calculated from equation (3):

$$IEC\left(meq \cdot g^{-1}\right) = \frac{C_{NaOH} \times V_{NaOH}}{M_s} \quad (3)$$

where C_{NaOH} and V_{NaOH} are the molar concentration and volume of the NaOH solution, respectively, M_s is the dry mass of the membrane.

The proton conductivity of the membranes was investigated by an AC impedance spectroscopy in the frequency range of 1 Hz and 1MHz. The prepared membranes were assembled in a two-electrode, custom-built, open-frame clamp. The humidity was controlled by deionized water (100% RH) and saturated $MgCl_2$ solutions (~33% RH). Each sample was tested in a controlled environment until the

impedance was constant. The membrane conductivity was calculated using equation (4):

$$\sigma = \frac{L}{RS} \tag{4}$$

where σ is the proton conductivity ($S \cdot cm^{-1}$), L is the distance between two electrodes (cm), R is the measured resistance (Ω), S is the superficial area (cm^2).

The activation energy (E_a) value of the samples was obtained by the least square fitting of the Arrhenius diagram. *Ea* was calculated using equation (5):

$$\sigma = \frac{ne^2 D_0 exp\left(\frac{\Delta S_m}{k}\right)}{kT} exp\left(\frac{-E_a}{kT}\right) \rightarrow \sigma = \frac{\sigma_0}{T} exp\left(\frac{-E_a}{kT}\right) \tag{5}$$

where n is the number of carriers, e is the charge of the carriers, D_0 is constantly associated with the proton conduction mechanism, ΔS_m is the entropy, σ_0 is a preexponential factor, k is the Boltzmann constant, E_a is the activation energy of the proton hopping, and T is the absolute temperature in kelvin.

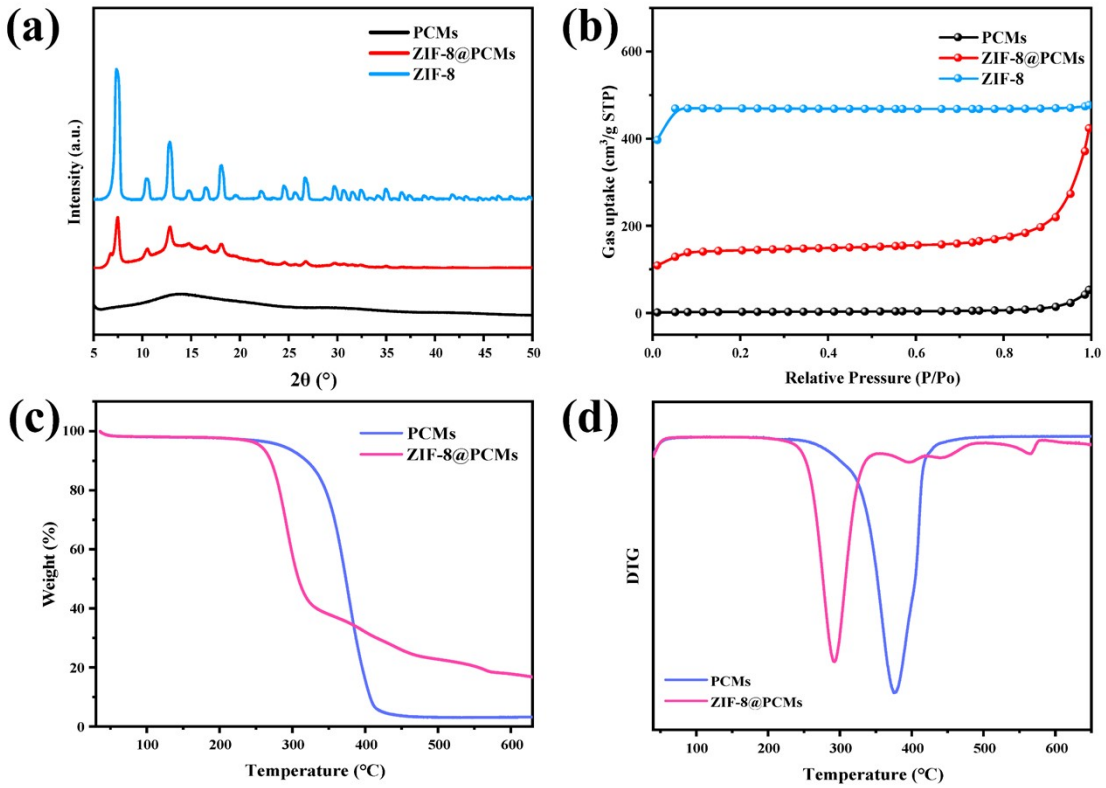

Fig. S2 (a) XRD patterns, (b) Nitrogen sorption isotherms of PCMs, ZIF-8@PCMs, and ZIF-8, (c, d) TGA and DTG curves of PCMs and ZIF-8@PCMs.

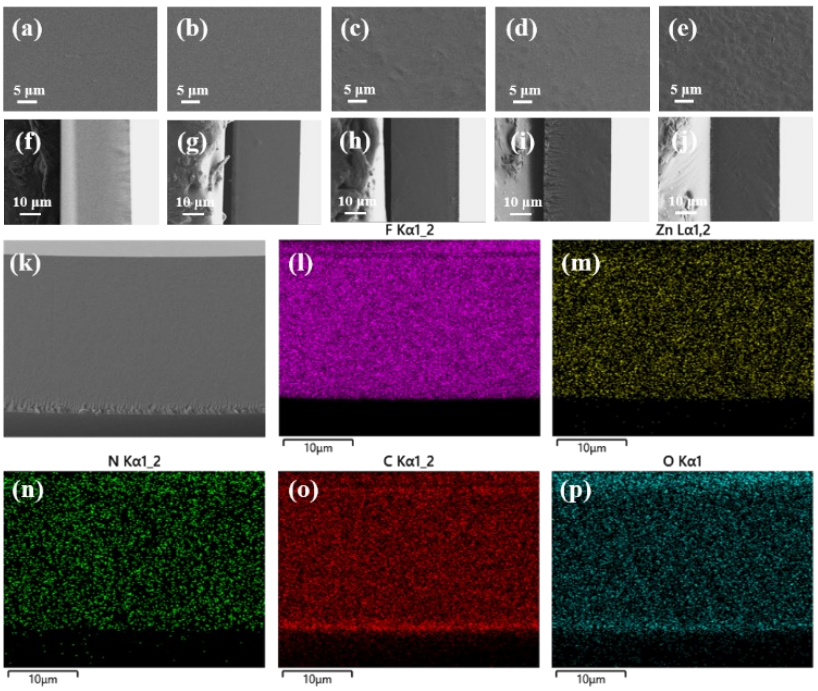

Fig. S3 The surface and cross-section SEM images of the (a, f) recast Nafion membrane, (b, g) Nafion/ZIF-8@PCMs-0.5, (c, h) Nafion/ZIF-8@PCMs-1, (d, i) Nafion/ZIF-8@PCMs-2, (e, j) Nafion/ZIF-8@PCMs-4 membranes. (k-p) Element mapping images of Nafion/ZIF-8@PCMs-1 composite membrane showing the presence of F, Zn, N, C and O elements.

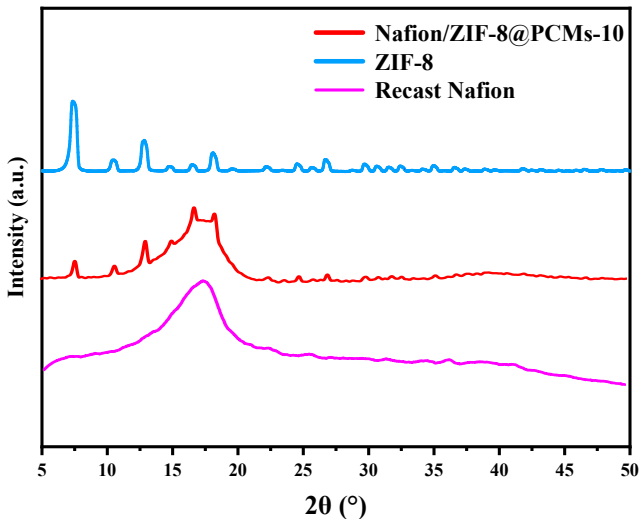

Fig. S4 XRD patterns of ZIF-8, recast Nafion, and Nafion/ZIF-8@PCMs-10.

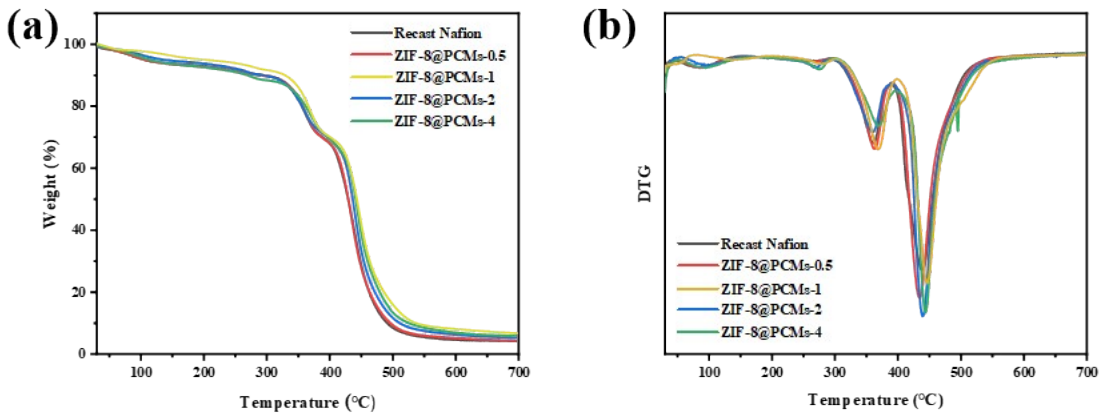

Fig. S5 (a) TGA and (b) DTG curves of the recast Nafion membrane and Nafion/ZIF-8@PCMs-x composite membranes.

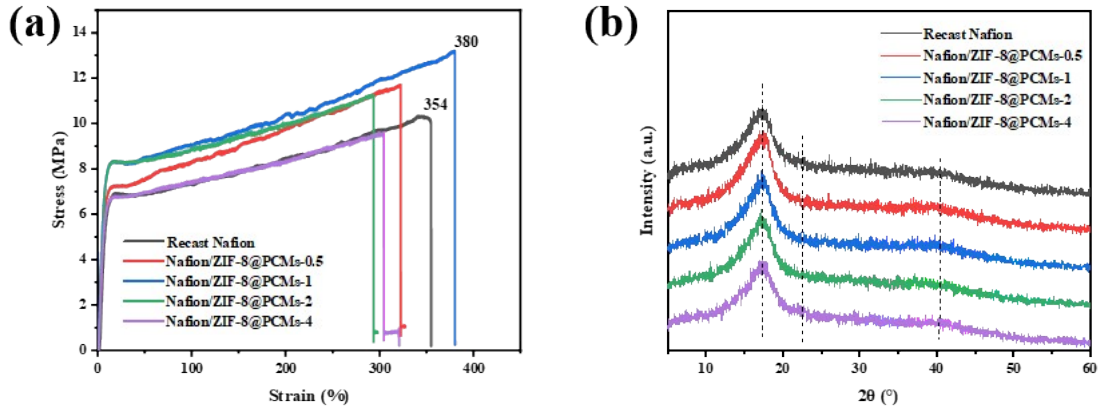

Fig. S6 (a) stress-strain and (b) XRD curves of the recast Nafion membrane and Nafion/ZIF-8@PCMs-x composite membranes.

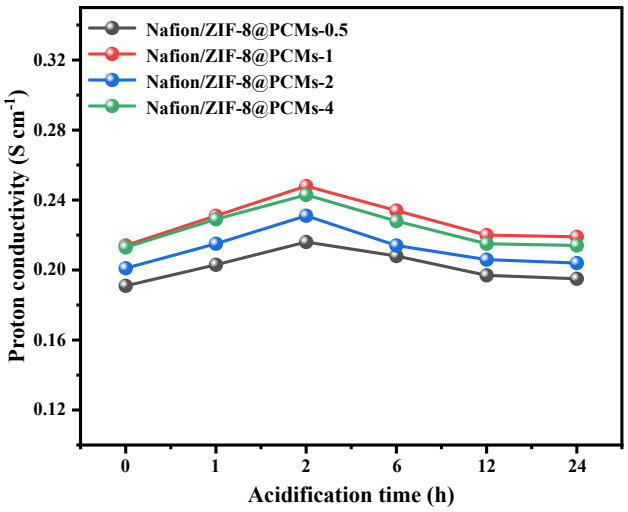

Fig. S7 Proton conductivities of the Nafion/ZIF-8@PCMs-X composite membranes after different acidification treatment time.

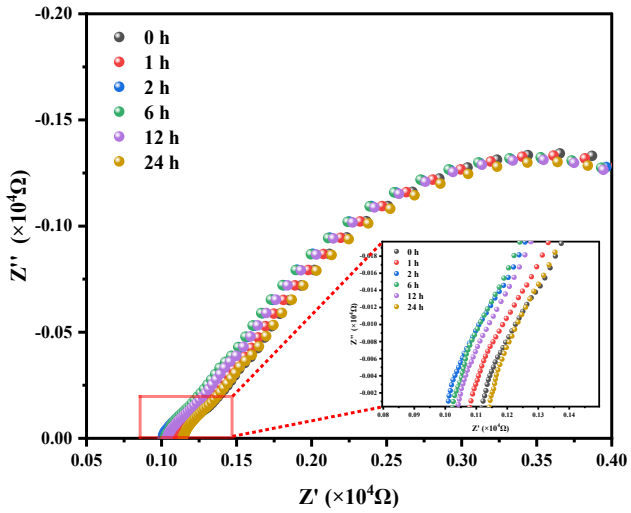

Fig. S8 Nyquist plots of the Nafion/ZIF-8@PCMs-1 membrane after different acidification treatment time.

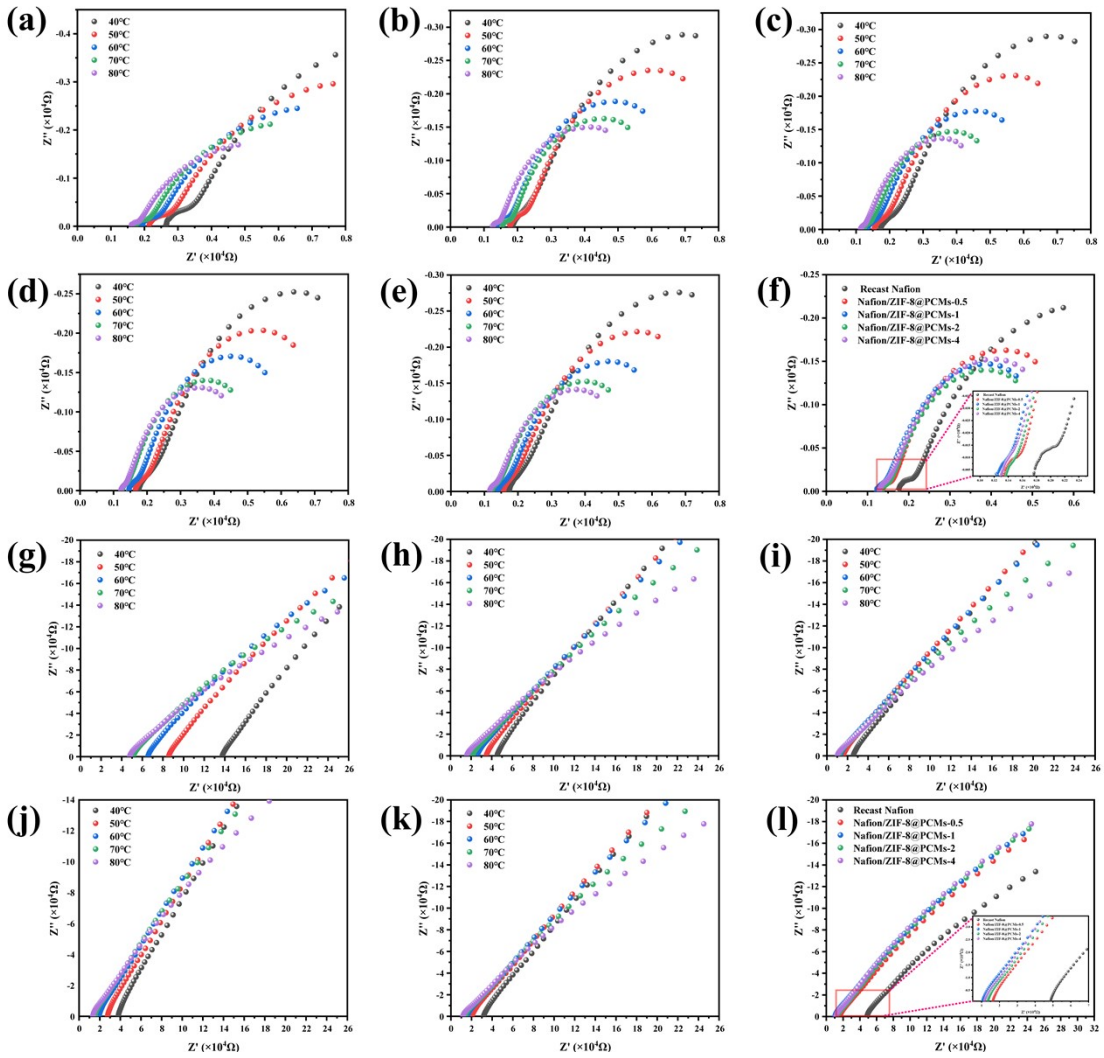

Fig. S9 Nyquist plots of different membranes at (a-f) 100% RH and (g-l) 33% RH. (a, g) Recast Nafion, (b, h) Nafion/ZIF-8@PCMs-0.5, (c, i) Nafion/ZIF-8@PCMs-1, (d, j) Nafion/ZIF-8@PCMs-2, (e, k) Nafion/ZIF-8@PCMs-4, (f, l) Nyquist plots of recast Nafion and Nafion/ZIF-8@PCMs-X composite membranes at 80 ℃ and 70 ℃.

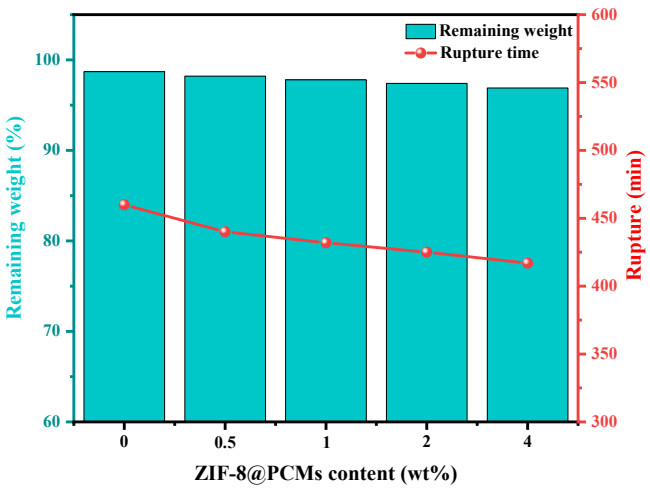

Fig. S10 Oxidative stabilities of recast Nafion and Nafion/ZIF-8@PCMs-X composite membranes.

As shown in **Fig. S10**, the residual weight after 1 h treatment and the time elapsed until the membrane began to break are summarized. Both the Nafion and hybrid membranes exhibit good oxidation resistance due to the low weight loss of less than 5% and long break time of more than 6 h, suggesting their good chemical durability. The introduction of ZIF-8@PCMs can slightly diminish the oxidative stability, which may because the high water absorption makes the polymer more susceptible to oxidative radical attack.

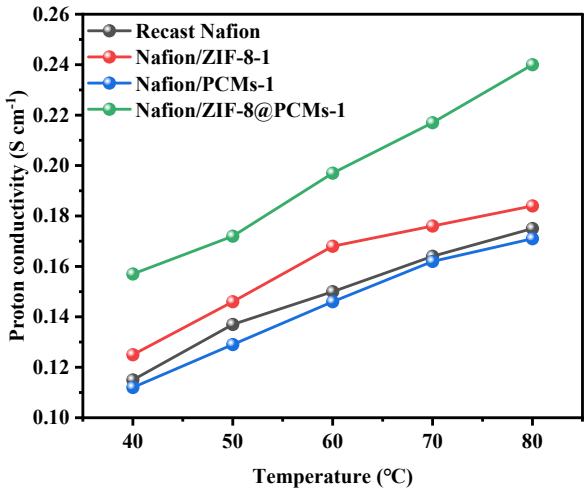

Fig. S11 Proton conductivities of the recast Nafion and composite membranes incorporated with different fillers under various temperatures.

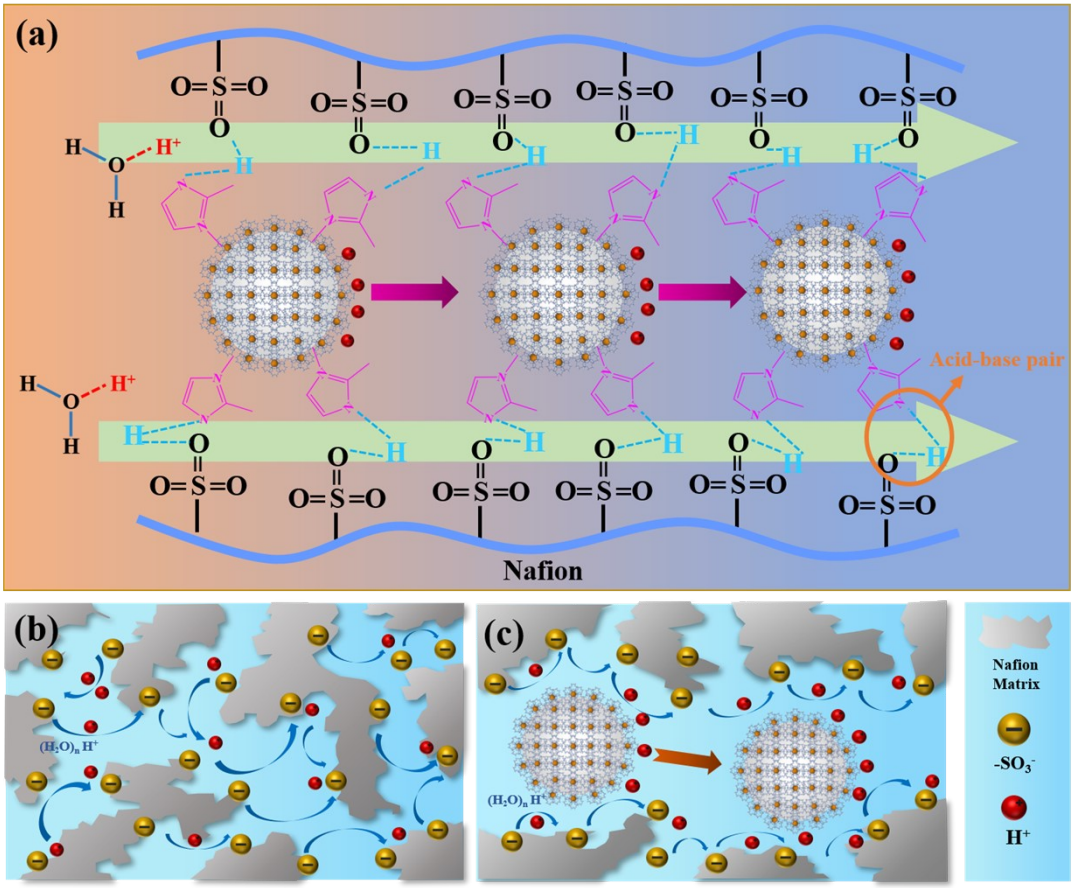

Fig. S12 (a) Schematic illustration of proton conduction in the Nafion/ZIF-8@PCMs composite membranes, (b, c) Nafion/ZIF-8@PCMs composite membrane with proton highways along ZIF-8@PCMs.

Table S1. Comparison of proton conductivity for ZIF-8@PCMs with other proton-conducting materials.

PEMs	Doping level (wt%)	Proton Conductivity (S cm^{-1})	Humidity Conditions (%)	Temperature (℃)	Reference
Nafion/phytic@MIL-101	12	0.0608	57.4	80	3
Nafion/ZIF-8@GO	1	0.21	40	80	4
Nafion/FDPA	10	0.0314	40	80	5
Nafion/NIM-SO_3	1	0.045	30	120	6
Nafion/Cage 3	5	0.27	95	90	7
Nafion/IL/MHSi	12	0.00541	30	30	8
Nafion/PWA/Silica	20	0.058	60	110	9
Nafion/PAA-PVA	5	0.144	95	60	10
Nafion/Amino-MIL-53	1	0.101	100	30	11
Nafion/Zn-MOF	5	0.00729	58	80	12
Nafion/sPES	2	0.223	100	80	13
Nafion/Bi-12	3	0.386	100	80	14
Nafion/APNB	10	0.076	100	80	15
Nafion/ZIF-8@PCMs	**1**	**0.24**	**100**	**80**	**This work**

References:

1 L. Y. Zhu, Y. C. Li, J. Y. Zhao, J. Liu, J. D. Lei, L. Y. Wang and C. B. Huang, *Chem. Commun.*, 2021, **57**, 9288-9291.

2 C. Yin, J. Li, Y. Zhou, H. Zhang, P. Fang and C. He, *ACS Appl. Mater. Interfaces*, 2018, **10**, 14026-14035.

3 Z. Li, G. W. He, B. Zhang, Y. Cao, H. Wu, Z. Y. Jiang and T. T. Zhou, *ACS Appl. Mater. Interfaces*, 2014, **6**, 9799-9807.

4 L. Yang, B. Tang and P. Wu, *J. Mater. Chem. A*, 2015, **3**, 15838-15842.

5 H. Zhang, Q. Hu, X. Zheng, Y. Yin, H. Wu and Z. Jiang, *J. Membr. Sci.*, 2019, **570-571**, 236-244.

6 L. G. Boutsika, A. Enotiadis, I. Nicotera, C. Simari, G. Charalambopoulou, E. P. Giannelis and T. Steriotis, *Int. J. Hydrog. Energy*, 2016, **41**, 22406-22414.

7 R. Y. Han and P. Y. Wu, *ACS Appl. Mater. Interfaces*, 2018, **10**, 18351-18358.

8 Y. Zhang, R. Xue, Y. Zhong, F. Jiang, M. Hu and Q. Yu, *Fuel Cells*, 2018, **18**, 389-396.

9 G. X. Xu, S. J. Xue, Z. Wei, J. Li, K. G. Qu, Y. Li and W. W. Cai, *Int. J. Hydrog. Energy*, 2021, **46**, 4301-4308.

10 A. Al Munsur, B. H. Goo, Y. Kim, O. J. Kwon, S. Y. Paek, S. Y. Lee, H. J. Kim and T. H. Kim, *ACS Appl. Mater. Interfaces*, 2021, **13**, 28188-28200.

11 X. L. Guo, Y. Fan, J. N. Xu, L. Wang and J. F. Zheng, *Ind. Eng. Chem. Res.*, 2020, **59**, 14825-14833.

12 H. F. Wang, Y. J. Zhao, Z. C. Shao, W. J. Xu, Q. Wu, X. L. Ding and H. W. Hou, *ACS Appl. Mater. Interfaces*, 2021, **13**, 7485-7497.

13 B. H. Goo, A. Al Munsur, O. Choi, Y. Kim, O. J. Kwon and T. H. Kim, *ACS Appl. Energy Mater.*, 2020, **3**, 11418-11433.

14 B. L. Liu, B. Hu, J. Du, D. M. Cheng, H. Y. Zang, X. Ge, H. Q. Tan, Y. H. Wang, X. Z. Duan, Z. Jin, W. Zhang, Y. G. Li and Z. M. Su, *Angew. Chem. Int. Ed.*, 2021, **60**, 6076-6085.

15 L. Liu, C. Wang, Z. F. He, D. Pan, B. B. Dong, S. Vupputuri and Z. H. Guo, *J. Power Sources*, 2021, **506**.